Stem Cell Research 56 (2021) 102528

Contents lists available at ScienceDirect

Stem Cell Research

journal homepage: www.elsevier.com/locate/scr

Lab Resource: Single Cell Line

Ataxia Telangiectasia iPSC line generated from a patient olfactory biopsy identifies novel disease-causing mutations

Hannah C. Leeson [a,*], Zoe Hunter [a], Harman Kaur Chaggar [a], Martin F. Lavin [b], Alan Mackay-Sim [c], Ernst J. Wolvetang [a,*]

[a] The University of Queensland, Australian Institute for Bioengineering & Nanotechnology (AIBN), St. Lucia, Brisbane, QLD 4072, Australia
[b] The University of Queensland, UQ Centre for Clinical Research (UQCCR), Herston, Brisbane, QLD 4006, Australia
[c] Griffith University, Griffith Institute for Drug Discovery (GRIDD), Nathan, Brisbane, QLD 4111, Australia

A B S T R A C T

Ataxia Telangiectasia is a rare autosomal recessive disorder caused by a mutated ATM gene. The most debilitating symptom of Ataxia Telangiectasia is the progressive neurodegeneration of the cerebellum, though the molecular mechanisms driving this degeneration remains unclear. Here we describe the generation and validation of an induced pluripotent stem cell (iPSC) line from an olfactory biopsy from a patient with Ataxia Telangiectasia. Sequencing identified two previously unreported disease-causing mutations in the ATM gene. This line can be used to generate 2D and 3D patient-specific neuronal models enabling investigations into the mechanisms underlying neurodegeneration.

Resource table

Unique stem cell line identifier	AIBNi014-A
Alternative name(s) of stem cell line	ONS-derived A-T iPSC, A-T HL iPSC
Institution	Australian Institute for Bioengineering and Nanotechnology
Contact information of distributor	Professor Ernst J Wolvetang: e.wolvetang@uq.edu.au
Type of cell line	iPSC
Origin	Human
Additional origin info required for human ESC or iPSC	Age: Child Sex: Female Ethnicity if known: Caucasian
Cell Source	Human olfactory neurosphere derived cells (ONS cells) GRIDD Neuro Bank ID # 906110003
Clonality	Clonal
Method of reprogramming	ReproRNA™-OKSGM (Stemcell Technologies): Non-integrating RNA reprogramming vector
Genetic Modification	No
Type of Genetic Modification	N/A
Evidence of the reprogramming transgene loss (including genomic copy if applicable)	N/A
Associated disease	Ataxia Telangiectasia (A-T)
Gene/locus	ATM gene: chr11:108,222,484–108,369,102 (GRCh38/hg38) Mutations:

(*continued on next column*)

Resource table (*continued*)

	Exon 10 homozygous splice acceptor variant: C>CT (NM_000051.3:c.1236-3dupT; RCV000159602.2), and **Exon 44 heterozygous frameshift (insertion) variant:** C>CTT (NM_000051.3:p.Arg2136fs/ c.6404_6405insTT; RCV000131770.2)
Date archived/stock date	9/11/2018
Cell line repository/bank	https://hpscreg.eu/cell-line/AIBNi014-A
Ethical approval	UQ HREC 2019000159 – Generation, differentiation and genetic manipulation of human induced pluripotent stem cells HREC/09/QRCH/103: Generation of neural progenitors from ataxia-telangiectasia patients

1. Resource utility

This human induced pluripotent stem cell (iPSC) line was generated from an Ataxia Telangiectasia (A-T) patient for generation of neuronal models to examine cerebellar neurodegeneration in A-T. If in vitro models recapitulate clinical observations, this line will be valuable for studies into the molecular mechanisms underpinning neurodegeneration in A-T.

* Corresponding authors.
E-mail addresses: h.leeson@uq.edu.au (H.C. Leeson), e.wolvetang@uq.edu.au (E.J. Wolvetang).

https://doi.org/10.1016/j.scr.2021.102528
Received 11 August 2021; Accepted 29 August 2021
Available online 1 September 2021

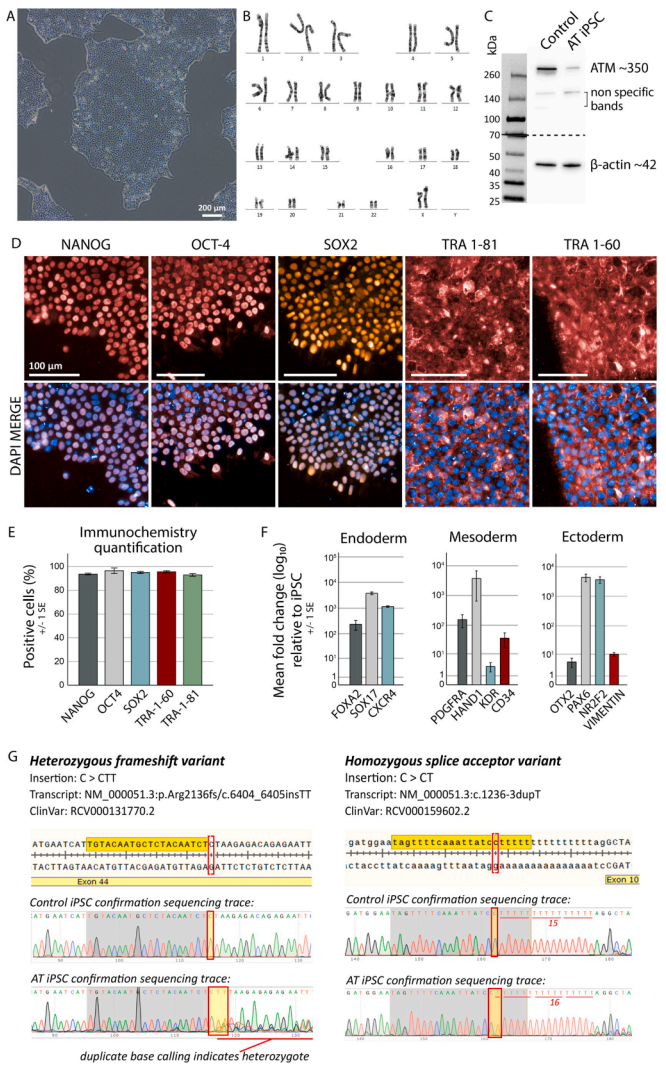

Fig. 1.

2. Resource details

Ataxia Telangiectasia (A-T) is a rare neurological and premature aging disorder caused by mutations in the ATM gene, responsible for orchestrating the DNA damage response pathway (Awasthi et al., 2015; Paull, 2015). Patients suffer a range of symptoms including immune defects, cancers, and a progressive neurodegeneration of the cerebellum (Rothblum-Oviatt et al., 2016). We have previously found making iPSCs from A-T patients to be technically challenging due to a ~100-fold reduction in reprogramming potential when compared to controls (Nayler et al., 2012), along with an increased predisposition to karyotypic abnormalities. Reprogramming from human olfactory neurosphere derived cells (ONS cells, an olfactory mucosal cell which may be differentiated to cells with neuronal-like characteristics (Stewart et al., 2013) had not been attempted previously and presented an additional confounding factor. Hence, we attempted reprogramming of five A-T ONS lines by transfection with the non-integrating ReproRNA™-OKSGM reprograming vectors (Stemcell Technologies). Of these, one A-T line (ID 906110003) successfully yielded 4 colonies, a success rate slightly less than our previously observed ~100 fold reduction compared to the anticipated 0.1% reported in the manufacturer guidelines. Whilst the lowest possible passage was used for reprogramming, ONS lines were between P8 and P12 and we expect that this could have had a detrimental impact on reprogramming efficiency.

Despite low reprogramming efficiency, the generated iPSCs demonstrated typical morphology (Fig. 1A) and a normal karyotype (46XX, Fig. 1B) was observed at 500bphs. Short tandem repeat (STR) analysis confirmed that the hiPSC profile matched that of the A-T patient (supplementary data). Western blot of A-T ONS-derived iPSCs confirmed that decreased expression of ATM protein was retained through the reprogramming process (Fig. 1C). Pluripotency was validated by immunochemistry for markers NANOG, OCT4, SOX2, TRA-1–81 and TRA-1–60 (Fig. 1D-E). Germ layer potential was assessed by directed differentiations to each lineage (Fig. 1F), and showed downregulation of pluripotency markers NANOG, OCT4 and SOX2 (data not shown), and upregulation of markers for endoderm (FOXA2, SOX17, CXCR4), mesoderm (PDGFRA, HAND1, KDR, CD34), and ectoderm (OTX2, PAX6, NR2F2, VIMENTIN).

The large size of ATM (69 exons) and the broad distribution of mutations within the ATM gene limits the feasibility of using Sanger to identify point mutations. Thus, whole genome sequencing (WGS) was undertaken to identify the mutation in ATM. Two novel disease-causing mutations were identified and confirmed by Sanger sequencing (Fig. 1G). A heterozygous frameshift variant resulting from an insertion of TT was identified in exon 44 (ClinVar: RCV000131770.2), and a homozygous splice acceptor variant caused by insertion of T at the splice acceptor site prior to exon 10 (ClinVar: RCV000159602.2). To the best of the authors knowledge, this represents the first time these mutations have been described in an A-T patient. Both mutations have previously been identified in germline cells as reported on ClinVar, though are not associated with or recorded as causing A-T. Additional information about the characterisation and validation of this A-T iPSC line is provided in Tables 1 and 2. Collectively, this data demonstrates the successful generation and quality of a pluripotent hiPSC line from an A-T patient with two novel disease-causing ATM mutations.

3. Materials and methods

3.1. Reprogramming ONS to iPSCs

Human olfactory neurosphere derived (ONS) cells were previously obtained as nasal biopsies from the olfactory mucosa of A-T patients with informed consent and ethical approval by the Queensland Children's Health Services Human Ethics Committee as described previously (Stewart et al., 2013). A-T patients were diagnosed at the A-T Clinic, University of Queensland Centre for Clinical Research, Brisbane, Australia. ONS cells were propagated as an adherent monolayer culture in DMEM/F12 supplemented with 10% foetal bovine serum (FBS), 1X Glutamax and 1X non-essential amino acids (NEAAs). Reprogramming was carried out using ReproRNA™-OKSGM (Stemcell Technologies); an RNA-based reprogramming vector expressing Glis1 and the four Yamanaka factors (OCT-3/4, KLF-4, SOX2 and c-Myc). Reprogramming was completed according to the manufacturer's instructions specific for fibroblasts, with modification of fibroblast medium to ONS medium. Cells were maintained in ReproTeSR until colony formation. Emerging colonies were individually selected, and medium was transitioned to mTeSR Plus. Subsequent passages were performed using 0.5 mM EDTA at a split ratio of 1:5–1:8 approximately every 5 days. Clumps were

Table 1
Characterization and validation.

Classification	Test	Result	Data
Morphology	Photography Bright field	Compact flat colonies with a well-defined smooth edge, containing cells with a high nucleus to cytoplasm ratio and prominent nucleoli	Fig. 1, panel A
Phenotype	Qualitative analysis: Immunocytochemistry staining	Positive staining of pluripotency markers: OCT4, SOX2, NANOG, TRA-1–60, TRA-1–81	Fig. 1, panel D
	Quantitative analysis	Robust endogenous expression of OCT4, NANOG, SOX2, TRA 1–60 and TRA 1–81 in >95% of cells	Fig. 1, panel E
Genotype	Karyotype (G-banding) and resolution	46XX, resolution 500bphs	Fig. 1, panel B
Identity	STR analysis	10 loci tested – matched	Provided
Mutation analysis (IF APPLICABLE)	WGS and Sanger confirmation sequencing	Mutation 1: Heterozygous frameshift variant resulting from an insertion of TT was identified in exon 44 (ClinVar: RCV000131770.2), (NM_000051.3:p.Arg2136fs/c.6404_6405insTT) Mutation 2: Homozygous splice acceptor variant caused by insertion of T at the splice acceptor site prior to exon 10 (ClinVar: RCV000159602.2) (NM_000051.3:c.1236-3dupT).	Fig. 1, panel G
	Western blot	A-T iPSC display a reduction in total protein content	Fig. 1, panel C
Microbiology and virology	Mycoplasma	Mycoplasma testing by Myco Alert Assay returned negative results with testing monthly	Not shown but available with author
Differentiation potential	Directed differentiation	Expression of endoderm markers (Sox17, Foxa2, Cxcr4), mesoderm markers (Pdgfra, Hand1, Kdr, CD34) and ectoderm markers (Otx2, Pax6, NR2F2, Vimentin).	Fig. 1, panel F
List of recommended germ layer markers	Germ layer expression validated by qPCR	Expression of endoderm markers (Sox17, Foxa2, Cxcr4), mesoderm markers (Pdgfra, Hand1, Kdr, CD34) and ectoderm markers (Otx2, Pax6, NR2F2, Vimentin).	Fig. 1, panel F
Donor screening (OPTIONAL)	HIV 1 + 2 Hepatitis B, Hepatitis C	N/A	N/A
Genotype additional info (OPTIONAL)	Blood group genotyping	N/A	N/A
	HLA tissue typing	N/A	N/A

plated without ROCK inhibitor on hESC qualified Matrigel (Corning) and were maintained in mTeSR Plus at 37 °C, 5% CO_2. All analysis was conducted on cells passage 5 onward.

3.2. Immunofluorescence staining

The iPSCs were fixed with 4% paraformaldehyde for 10 min at 4 °C before blocking and permeablisation for 1 h with 3% Bovine Serum Albumin (BSA) and 0.1% TritonX-100 in PBS. Pluripotency markers (Table 2) were incubated overnight at 4 °C, and secondary antibodies were incubated for 1hr at room temperature. Nuclei were counter-stained with 1 μg/ml DAPI or Hoechst.

3.3. Germ lineage differentiations

Directed differentiation was used to confirm potential for generation of three germ layers. Directed differentiations for each germ layer involved culturing the iPSCs in respective differentiation medium. For ectoderm differentiation, neural induction medium (1:1 DMEM/F12 and Neurobasal medium, 0.5X N2, 0.5X B-27, 1X GlutaMax, 0.5X NEAAs, 2.5 μg/mL insulin and 50 μM β-mercaptoethanol) with dual SMAD inhibition (10 μM SB431542 and 0.1 μM LDN-193189) was fed for 10 days. Endoderm differentiation used STEMdiff Definitive Endoderm Kit (Stemcell Technologies) for 5 days and mesoderm was fed with RPMI supplemented with 1X B-27 and 5 μM CHIR for 5 days. Differentiations were harvested for RNA and analysed by qPCR.

3.4. Quantitative PCR (qPCR)

RNA was extracted using Nucleospin RNA extraction kit (Macherey-Nagel) and cDNA was synthesised using BioRad iScript cDNA Synthesis kit. All qPCR reactions were performed in triplicate using PowerUp SYBR Green Master Mix (Thermo Fisher) and a BioRad CXF96 Real Time machine. Cycle conditions were 95 °C for 2 min, followed by denaturation (95 °C for 15 s), annealing (55–60 °C for 15 s) and extension (72 °C for 1 min) for 40 cycles. Results were expressed as double delta CT. Primers are listed in Table 2.

3.5. Karyotyping

The A-T iPSC line was karyotyped by Sullivan Nicolaides Pathology (Bowen Hills, Queensland), at a resolution of 500 bands per haploid set (bphs).

3.6. Short tandem repeat (STR) analysis

DNA was extracted from A-T iPSCs and the corresponding patient ONS line and underwent STR analysis (GenePrint-10) by the Australian Genome Research Facility in Melbourne.

3.7. Mycoplasma testing

Culture medium routinely underwent mycoplasma testing using MycoAlert Assay.

Declaration of Competing Interest

The authors declare that they have no known competing financial interests or personal relationships that could have appeared to influence the work reported in this paper.

Table 2
Reagents details.

	Antibodies used for immunocytochemistry/flow-cytometry			
	Antibody	Dilution	Company Cat #	RRID
Pluripotency Markers	Mouse Anti OCT4 IgG	1:100	Millipore Cat# MAB4419	RRID: AB_1977399
	Rabbit Anti SOX2 IgG	1:400	Cell Signaling Technology Cat# 23064	RRID: AB_2714146
	Mouse Anti NANOG IgG	1:2000	Cell Signaling Technology Cat# 4893	RRID: AB_10548762
	Mouse Anti Tra-1–60 IgG	1:200	Millipore Cat# MAB4360	RRID: AB_2119183
	Mouse Anti Tra-1–81 IgG	1:100	Millipore Cat# MAB4381	RRID:AB_177638
Secondary Antibodies	Goat Anti Mouse IgG H + L Alexa Fluor 647	1:500	Thermo Fisher Scientific Cat# A-21235	RRID: AB_2535804
	Goat Anti Mouse IgG H + L Alexa Fluor 488	1:500	Thermo Fisher Scientific Cat# A-11029	RRID: AB_2534088
	Goat Anti Rabbit IgG H + L Alexa Fluor 647	1:500	Thermo Fisher Scientific Cat# A-21245	RRID: AB_2535813
	Donkey Anti Mouse IgG H + L Alexa Fluor 568	1:500	Thermo Fisher Scientific Cat# A-10037	RRID: AB_2534013
	Primers			
	Target	Size of band (bp)	Forward/Reverse primer (5′-3′)	
Differentiation primers (qPCR)	SOX17 (endoderm)	94	GTGGACCGCACGGAATTTG/ GGAGATTCACACCGGAGTCA	
	FOXA2 (endoderm)	83	GGAGCAGCTACTATGCAGAGC/ CGTGTTCATGCCGTTCATCC	
	CXCR4 (endoderm)	61	GCCTTACTACATTGGGATCAG/ CCCTTGCTTGATGATTTCCA	
	PDGFRA (mesoderm)	92	GTCTTCTCACAGGGCTGAG/ TGAATTCAGCTGCACAACC	
	HAND1 (mesoderm)	170	CCATGCTCCACGAACCCTTC/ CCTGGCGTCAGGACCATAG	
	KDR (mesoderm)	81	GTCACTTTGTGCAAGATACCC/ GTAAAGCCCTTCTTGCTGTC	
	CD34 (mesoderm)	89	CCAACAGAACAGAAATTTCCAG/ CTCAGTGAAATCTAGGATCCC	
	OTX2 (ectoderm)	81	CCAGACATCTTCATGCGAG/ TCGATTCTTAAACCATACCTGC	
	PAX6 (ectoderm)	320	ACACACTTGAGCCATCACCA/ TTCCACGGGGCTCGAATATG	
	NR2F2 (ectoderm)	151	TCATGGGTATCGAGAACATTTGC/ TTCAACACAAACAGCTCGCTC	
	VIMENTIN (ectoderm)	81	TCCACGAAGAGGAAATCCA/ CAGGCTTGGAAACATCCAC	
House-Keeping Gene (qPCR)	GAPDH AGCCACATCGCTCAGACAC/ GCCCAATACGACCAAATCC	66		
A-T mutation confirmation (Sanger seq)	**Mutation 1:** Heterozygous frameshift variant	323	AAATTTTGTCCTTTGGTGAAGC/ TGATCACAGCCACCAAGTCT	
	Mutation 2: Homozygous splice acceptor variant	309	CAGCTAGCCAAACGTTGACA/ GCTGTTGGGGTAGAAGCTGA	

Acknowledgements

This work was supported by funding from the National Health and Medical Research Council (EW and ML), and from the Australian Department of Health (AMS). The authors also extend thanks to BrAshA-T for their support of this project.

Appendix A. Supplementary data

Supplementary data to this article can be found online at https://doi.org/10.1016/j.scr.2021.102528.

References

Awasthi, P., Foiani, M., Kumar, A., 2015. ATM and ATR signaling at a glance. J. Cell Sci. 128 (23), 4255–4262.
Paull, T.T., 2015. Mechanisms of ATM activation. Annu. Rev. Biochem. 84 (1), 711–738.
Rothblum-Oviatt, C., Wright, J., Lefton-Greif, M.A., McGrath-Morrow, S.A., Crawford, T. O., Lederman, H.M., 2016. Ataxia telangiectasia: a review. Orphanet. J. Rare Dis. 11 (1) https://doi.org/10.1186/s13023-016-0543-7.
Nayler, S., et al., Induced pluripotent stem cells from ataxia-telangiectasia recapitulate the cellular phenotype. Stem Cells Transl. Med., 2012. 1(7): 523–535.
Stewart, R., et al., A patient-derived olfactory stem cell disease model for ataxia-telangiectasia. Hum. Mol. Genet., 2013. 22(12): p. 2495–509.